TENTH AUSTRALASIAN FLUID MECHANICS
CONFERENCE - UNIVERSITY OF MELBOURNE
11-15 DECEMBER 1989

HYPERVELOCITY FLOW IN AXISYMMETRIC NOZZLES

P.A. JACOBS and R.J. STALKER

Department of Mechanical Engineering
The University of Queensland, St. Lucia, Qld. 4067
AUSTRALIA

ABSTRACT.

We describe a simple procedure for the design of axisymmetric supersonic nozzles for use in reflected-mode shock tunnels. This method has been used to design a moderate Mach number (M = 4) nozzle and a high Mach number (M = 10) nozzle. Both nozzles have been calibrated by measuring the pitot profiles near the nozzle exit planes and, although the M = 4 nozzle performs well, the M = 10 appears to have reached a Mach number - pressure limit in which the unsteady nozzle boundary layers significantly affect the test flow.

INTRODUCTION.

A new generation of aerospace planes is currently being developed. These vehicles will be powered by air-breathing engines and so spend a considerable fraction of their flight accelerating through the atmosphere. This means that high speed (v ~ 3-7km/s) aerodynamics will again become a focus for fluid dynamic researchers.

Experimental facilities capable of providing test flows at these speeds supply a pulse of test gas that lasts only a few milliseconds. To make the best use of the high enthalpy test gas, it is expanded to a high-speed uniform and parallel flow. For the shock tunnel facility T4 (Stalker & Morgan 1988), this is achieved by using an axisymmetric nozzle in which the gas is initially allowed to expand through a conical section and is then redirected by the contoured part of the nozzle wall to produce a uniform test flow at the nozzle exit plane.

Impulse facilities such as T4 typically operate at total enthalpies (H_s) of 10 - 30 MJ/kg with associated stagnation temperatures (T_s) of 5000 - 12000 K and stagnation pressures (P_s) of 40 MPa. At these conditions there is a strong coupling between the chemical reactions of the dissociated air and the axisymmetric gas flow. This coupling complicates the design calculations significantly. However axisymmetric nozzles for non-reflecting shock tunnels have been designed using the method of characteristics (MOC) with chemical reactions by Mudford *et al* (1980). In their design they note that the contour shapes computed for a chemically reacting flow were similar to that computed for a perfect gas with a suitably chosen ratio of specific heats, γ.

This leads us to approach the design process in a simple fashion and treat the total flow as two relatively simple flows patched together. We treat the early expansion of the test gas in the conical section as a quasi-one-dimensional flow with finite-rate chemical kinetics. At the exit of this cone we assume that the flow is a uniform source flow and that the chemical reactions are frozen. We then treat the flow in the contoured section as axisymmetric flow of a perfect gas where γ has been chosen to approximate a chemically reacting flow over the same expansion. The MOC calculation of the flow in the contoured section is then the "standard" perfect gas procedure described in Liepmann & Roshko (1957).

This approach has been used to design a nozzle with exit Mach number, M = 4 for use in supersonic combustion studies (see figure 1a). Its performance in terms of flow uniformity appears to be adequate. A high Mach number (M = 10) nozzle was also constructed (see figure 1b). It has a two-stage initial expansion to reduce the time required for the test flow to reach steady state. Unfortunately, for nozzle stagnation pressure P_s < 40 MPa, the boundary layers that develop on the nozzle wall significantly affect the uniformity of the flow.

MACH 4 NOZZLE.

We will consider the design of a specific nozzle with M = 4 and a throat diameter of 25.0mm, at nominal stagnation conditions P_s = 30.4MPa, H_s = 16.2MJ/kg (T_s = 8000K). The conceptual layout of the nozzle is shown in figure 2. For computational convenience, we set the origin of the axial coordinate, x, at the start of the conical expansion.

For the initial conical expansion, we choose a cone half-angle of 12^0 and we assume the flow to be a uniform source flow at the end of this section (x = 98mm). Zonars (1967) indicated that throats with a constant area section with length equal to the throat diameter produced "excellent high temperature source flow characteristics when measured in conical nozzles". Hence we do not analyse the transonic flow near the throat as done in a number of other studies (*e.g.* Sivells 1978).

The flow in the conical section is strongly influenced by the chemical reactions associated with the dissociation and recombination of the molecules in test gas. We treat this flow as a quasi-one-dimensional flow with finite rate chemical kinetics. Computations are performed with a FORTRAN program NENZF (Lordi *et al* 1964). The stagnation region (labelled 1 in figure 2) and the subsonic flow up to the throat is considered to be in chemical equilibrium but, once the program steps into the conical expansion, a nonequilibrium chemistry model is used.

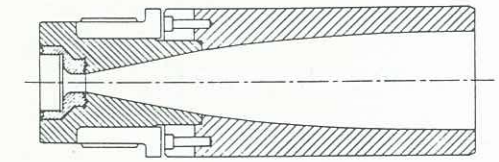

M = 4

100mm

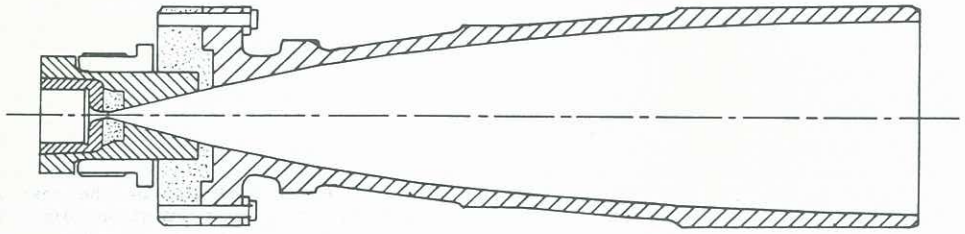

M = 10

Figure 1.

M = 4 and M = 10 axisymmetric nozzles constructed for the T4 shock tunnel facility.

We use the flow properties (M and γ) at the end of the conical section as the starting point for the MOC calculation of the flow in region 3 (source flow), region 4 (transition from source flow to parallel flow) and region 5 (parallel and uniform flow). The gas flow is considered to be chemically frozen and a value of M at the end of the conical expansion is calculated using an estimate of the speed of sound $a = (\gamma\ S\ \mathcal{R}_0\ 1000\ T)^{0.5}$, where S is the sum of the species concentrations (mole/gm-mixture) $\mathcal{R}_0 = 8.314$ J/gm-mole/K and T is the static temperature in K. Here a = 1380 m/s. The computation was performed with the aid of the program "MOC" documented in Jacobs (1988). The inlet boundary is specified as a uniform source flow with $M_A = v/a = 2.804$ and $\gamma = 1.334$. Only 12 points were used on the inlet boundary as the program retains all of the mesh data in the memory of the microcomputer. We believe this to be sufficient because Schurmeier (1959) indicates that a 10 point mesh produced a 0.1% error in exit height for a two- dimensional nozzle calculation. The Mach number on the axis at point C (in figure 2) is computed to be $M_c = 4.12$. We then step along the axis downstream of point C and compute the flow field in region 4 by proceeding upstream along characteristics such as CA.

Once the characteristic mesh is generated, a streamline can be interpolated through the mesh, starting at point A and finishing where it intersects the characteristic CD. The data points on the interpolated streamline are then used in a spline fitting routine to define the nozzle wall as a cubic spline with eight knots and specified end slopes. See table 1 for the wall coordinates. A boundary layer modification was added to give a total wall radius

$$r_{total} = r_{inviscid} + \frac{x}{511}\,\delta^*_{exit}$$

where δ^*_{exit} was estimated to be 1.4mm.

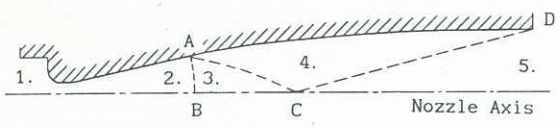

Figure 2. Conceptual view of a hypersonic nozzle.
1. Stagnation region.
2. Transition to source flow.
3. Source flow region.
4. Transition to parallel flow.
5. Uniform flow parallel to nozzle axis.

Calibration of the Mach 4 Nozzle.

The performance of the nozzle was evaluated by measuring the pitot pressure, P_{pitot}, at a plane normal to the nozzle axis and located a distance z = 120mm downstream of the nozzle exit plane. Each pitot probe was fitted with a PCB-112 piezo-electric pressure transducer which measured the stagnation pressure behind a detached shock that formed over the upstream face of the probe. Several probes were mounted in a rake and a number of shots of the shock tunnel were required to build up each pitot profile.

Figure 3 shows the time history of some of the pressures. The "raw" traces for both P_s and P_{pitot} (figure 3A) show the impulsive start and subsequent decay associated with "under-tailored" operation of the shock-tube. In this mode, the shock that compresses the test gas reflects in such a way as to allow the compressed test gas to expand back up the shock-tube. This reduces P_s during the test flow time but delays contamination of the test gas (air) by the driver gas (helium). To eliminate the time variation from our pitot pressure measurements, we normalize P_{pitot} by P_s with a suitable time delay (here 0.2 msec) and filter (time constant = 0.05msec). The normalized traces for 4 pitot probes are shown in figure 3B. We then discard the first 0.5msec of the trace which contains the starting pulse and measure the mean value over the next 0.5msec. This mean value, together with an estimate of its variation over the test time is plotted as a single point on the pitot pressure profile.

Figure 4 shows pitot profiles for a nominal stagnation pressure P_s = 13Mpa and three enthalpies H_s = 16, 8.8 and 6.6MJ/kg. There is some fall-off at the edge of the core flow but this is due to the expansion fan from the trailing edge of the nozzle propagating into the test flow. The performance of the nozzle appears to be satisfactory but we cannot measure how parallel the flow is because the pitot probes are insensitive to small changes in flow angle.

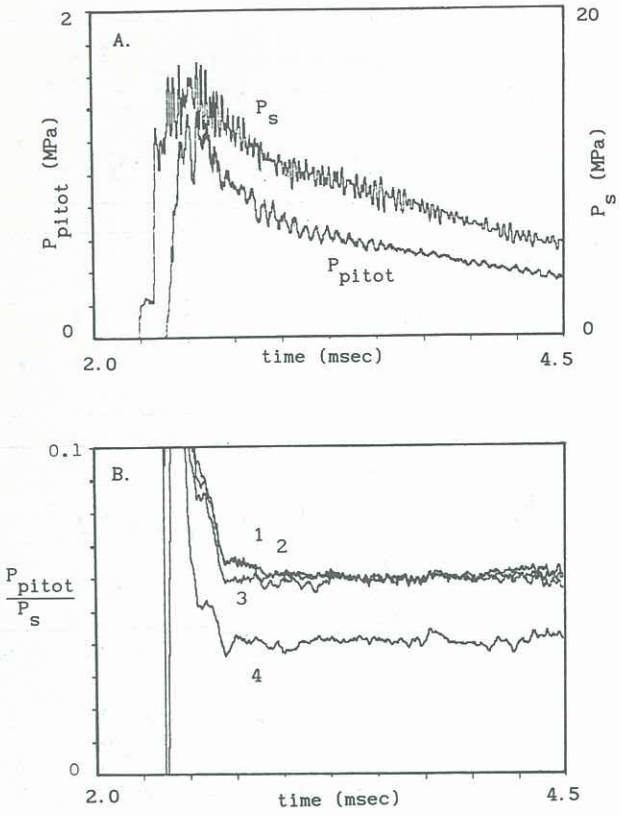

Figure 3. Pressure-time traces for the M = 4 nozzle. P_s = 13MPa, H_s = 16MJ/kg.
A. "Raw" stagnation and pitot pressure.
B. Normalized pitot pressure.

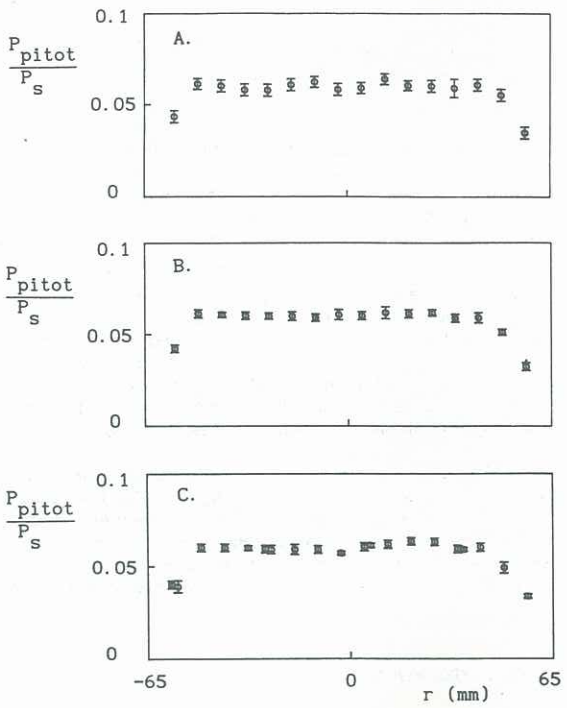

Figure 4. Pitot pressure profiles for the M = 4 nozzle. P_s = 13Mpa, H_s = 120mm.
A. H_s = 6.6MJ/kg
B. H_s = 8.8MJ/kg
C. H_s = 16MJ/kg

MACH 10 NOZZLE.

The starting process for the flow in a hypersonic nozzle involves the propagation of primary and secondary shock waves and an unsteady expansion through the nozzle. Smith (1966) has shown that the time, t_s, required for the flow to approach steady state is dominated (in general) by time taken to sweep the upstream head of the unsteady expansion out of the nozzle. For conical nozzles with fixed divergence angle, t_s increases rapidly with M. To reduce t_s (and hence reduce the amount of gas consumed in the starting process) for a nozzle with large M, we may increase the divergence angle of the initial conical section. However, if the angle is too large, the flow will separate.

We will now describe a nozzle with M = 10 and a two-stage initial expansion designed to avoid flow separation. Immediately after the throat (diameter d = 6mm), the gas is expanded through a cone with a 15° half-angle. From previous experience, this was the largest divergence that would give reasonably uniform flow. Starting at x = 2d, the half-angle is incremented a further 5° (in 1° steps) over the next 8d. The resulting conical section (20° half-angle) is then truncated further downstream (at x = 47.7mm) and a contoured section added to straighten the flow.

This contoured section was designed in much the same way as that for the M = 4 nozzle but at nominal conditions H_s = 35MJ/kg (T_s = 11000K) and P_s = 30MPa. NENZF was used to compute M = 3.69 and γ = 1.41 at the start of the contoured section. This relatively high value of γ is a result of the large fraction of monatomic species found at the end of the conical expansion. Coordinates for the complete contour are given in table 2. No boundary layer modification was added to these inviscid coordinates. To reduce the length of the fabricated nozzle without affecting the usable test core, we truncated the nozzle at the x-station where the characteristic CD intersects the estimated position of the edge of the boundary layer. Because of the large exit Mach number, the fabricated nozzle was much shorter (l = 1036mm) than the full inviscid contour (l = 1777mm).

Calibration of the Mach 10 Nozzle.

As for the M = 4 nozzle, the performance of the M = 10 nozzle was evaluated by measuring the pitot pressure downstream of the nozzle exit plane. Figure 5 shows pitot profiles for two flow conditions. Profile A (P_s = 20MPa, H_s = 30MJ/kg) indicates that the nozzle is **not** performing well and may even have a conical shock present in the flow. We performed some finite- difference computations with a parabolized Navier- Stokes program and obtained similar pitot profiles when a shock was present. Profile B (z = 369mm) shows a better profile, possibly because the shock has passed out of the test flow core at this axial position. The expansion propagating from the trailing edge of the nozzle has reduced the diameter of the test core at this axial position. We note also that the normalized pitot traces for this condition changed continuously through the test time. This indicates that the boundary layers on the nozzle wall did not reach steady

state.

Operating the nozzle at higher pressure (see profile C, P_s = 40MPa) significantly improves the flow uniformity but there is still a depression in the centre of the pitot profile. We suspect that this improvement in nozzle performance is a result of reducing the boundary layer that grows along the nozzle wall. For profiles A and C, we estimate the total boundary layer thickness at the exit plane to be δ_A = 82mm and δ_C = 58mm. These values scale as $Re^{-1/2}$ which indicates that the boundary layer is laminar. Assuming that displacement thickness $\delta^* = 0.33\,\delta$, the effective area ratio of the nozzle is reduced from the design value 2290 to 1450 and 1680 for profiles A and C respectively. Values of pitot pressure computed with NENZF for these effective area ratios are shown as dashed lines in figure 5.

In conclusion, it appears that our design approach is satisfactory for hypervelocity nozzles with moderate exit Mach number. However, nozzles with high values of exit Mach number need to be operated at sufficiently high pressure to ensure that their boundary layers do not disturb the core flow.

ACKNOWLEDGEMENTS.

We wish to thank Dr. Peter Killen and Ken Dudson for constructing the M = 10 nozzle, Denis Sussmilch for constructing the M = 4 nozzle and Craig Brescianini for performing finite-difference calculations of flow in the M = 10 nozzle. This work was supported by ARC and NASA (under grant NAGW-674).

REFERENCES.

Jacobs, P.A. 1988 "An interactive graphics program for computer assisted calculation of isentropic flows." Report 7/88, Department of Mechanical Engineering, University of Queensland.

Liepmann, H.W. & Roshko, A. 1957 *Elements of Gasdynamics.* John Wiley & Sons.

Lordi, J.A., Mates, R.E. & Moselle, J.R. 1966 "Computer program for the numerical solution of nonequilibrium expansions of reacting gas mixtures." NASA-CR-472.

Mudford, N.R., Stalker, R.J. & Shields, I. 1980 "Hypersonic nozzles for high enthalpy nonequilibrium flow." *Aeronautical Quarterly* May 1980, 113-131.

Schurmeier, H.M. 1959 "Design and operation of a continuous-flow hypersonic wind tunnel using a two- dimensional nozzle." AGARDograph 38.

Sivells, J.C. 1978 "A computer program for the aerodynamic design of axisymmetric and planar nozzles for supersonic and hypersonic wind tunnels." AEDC-TR-78-63.

Smith, C.E. 1966 "The starting process in a hypersonic nozzle." *J. Fluid Mech.* **24**, 625-640.

Stalker, R.J. & Morgan, R.G. 1988 "The University of Queensland free piston shock tunnel T4 - Initial operation and preliminary calibration."

Zonars, D. 1967 "Nonequilibrium regime of airflows in contoured nozzles: theory and experiment." *AIAA J.* **4**(1), 57-63.

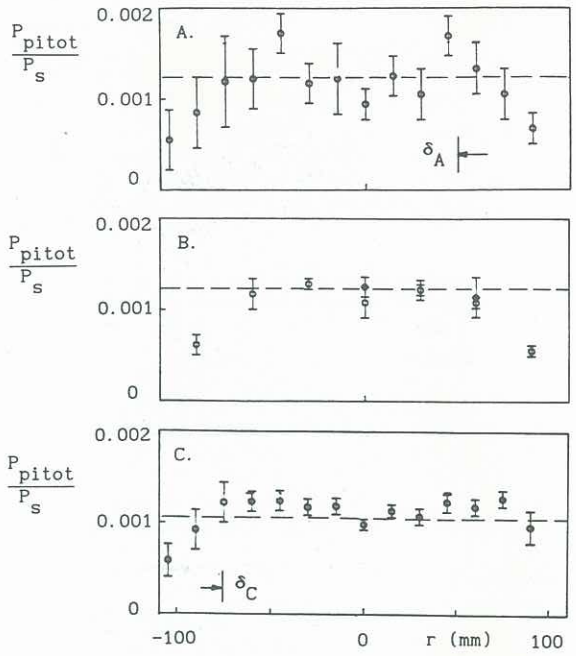

Figure 5. Pitot pressure profiles for the M = 10 nozzle. The dashed lines indicate the NENZF computed level with $\delta^*/\delta = 0.33$.
A. P_s = 20Mpa, H_s = 30MJ/kg, z = 139mm.
B. P_s = 20Mpa, H_s = 30MJ/kg, z = 369mm.
C. P_s = 40Mpa, H_s = 25MJ/kg, z = 139mm.

Table 1. Coordinates for the M = 4 inviscid contour. Points with x ≥ 98mm are knots on a cubic spline.

x (mm)	$r_{inviscid}$(mm)	comment (slope)
0.0	12.5	start of 12° cone
98.43	33.43	start of contour (0.2126)
157.48	44.45	
216.54	52.79	
275.59	58.56	
334.65	62.30	
393.70	64.66	
452.76	65.88	
511.81	66.07	end of contour (-0.0048)

Table 2. Coordinates for the M = 10 inviscid contour. Points with x ≥ 47mm are knots on a cubic spline.

x (mm)	$r_{inviscid}$(mm)	comment (slope)
0.0	3.00	start of 15° cone
12.0	6.24	end of 15° cone
15.0	7.09	
18.0	8.03	
21.0	9.00	
24.0	10.03	start of 20° cone
47.70	18.66	start of contour (0.3640)
294.78	74.51	
541.85	104.66	
788.93	121.57	
1036.00	132.76	
1283.08	139.13	
1530.16	142.44	
1777.23	143.55	end of contour